



## Short communication

Performance of  $\text{LiNi}_{0.5}\text{Mn}_{1.5}\text{O}_4$  prepared by solid-state reactionZhaoyong Chen<sup>a,\*</sup>, Huali Zhu<sup>a</sup>, Shan Ji<sup>b</sup>, Vladimir Linkov<sup>b</sup>, Jianli Zhang<sup>a</sup>, Wei Zhu<sup>a</sup><sup>a</sup> Institution of Materials Science and Engineering, Department of Physics and Electronic Sciences, Changsha University of Science and Technology, Changsha 410076, China<sup>b</sup> South Africa Institute for Advanced Materials Chemistry, University of the Western Cape, Bellville 7535, South Africa

## ARTICLE INFO

## Article history:

Received 24 July 2008

Received in revised form 9 October 2008

Accepted 1 November 2008

Available online 7 November 2008

## Keywords:

 $\text{LiNi}_{0.5}\text{Mn}_{1.5}\text{O}_4$ 

Spinel

Cathode materials

Lithium ion battery

## ABSTRACT

$\text{LiNi}_{0.5}\text{Mn}_{1.5}\text{O}_4$  was prepared through a solid-state reaction using various Ni precursors. The effect of precursors on the electrochemical performance of  $\text{LiNi}_{0.5}\text{Mn}_{1.5}\text{O}_4$  was investigated.  $\text{LiNi}_{0.5}\text{Mn}_{1.5}\text{O}_4$  made from  $\text{Ni}(\text{NO}_3)_2 \cdot 6\text{H}_2\text{O}$  shows the best charge–discharge performance. The reversible capacity of  $\text{LiNi}_{0.5}\text{Mn}_{1.5}\text{O}_4$  is about  $145 \text{ mAh g}^{-1}$  and remained  $143 \text{ mAh g}^{-1}$  after 10 cycles at 3.0–5.0 V. The XRD results showed that the precursors and the dispersion methods had significant effect on their phase purity. Pure spinel phase can be obtained with high energy ball-milling method and  $\text{Ni}(\text{NO}_3)_2 \cdot 6\text{H}_2\text{O}$  as precursor. Trace amount of NiO and  $\text{Li}_2\text{MnO}_3$  phase were detected in  $\text{LiNi}_{0.5}\text{Mn}_{1.5}\text{O}_4$  with manual-mixture method and using  $\text{Ni}(\text{CH}_3\text{COO})_2 \cdot 6\text{H}_2\text{O}$ , NiO and  $\text{Ni}_2\text{O}_3$  as precursors.

© 2008 Elsevier B.V. All rights reserved.

## 1. Introduction

$\text{LiNi}_{0.5}\text{Mn}_{1.5}\text{O}_4$  has been considered as promising alternatives to  $\text{LiCoO}_2$  cathode materials in Li-ion secondary batteries, which possesses highly reversible discharge capacity at 5 V, high energy density and power density [1–3]. In  $\text{LiNi}_{0.5}\text{Mn}_{1.5}\text{O}_4$ ,  $\text{Mn}^{4+}$  forms the lattice frame of crystal and  $\text{Ni}^{2+}$  is responsible for redox, which could stabilize this compound and facilitate intercalation/deintercalation and diffusion of Li-ions during cycling [4–6]. However, the solid-state reaction used commonly to prepare  $\text{LiNi}_{0.5}\text{Mn}_{1.5}\text{O}_4$  is not adequate to control the composition of Ni and Mn, and produces impurity in the form of NiO. The capacity of  $\text{LiNi}_{0.5}\text{Mn}_{1.5}\text{O}_4$  prepared through solid-state reaction is only  $120 \text{ mAh g}^{-1}$ . In order to get high purity spinel phase, various synthesis methods had been developed. Pure  $\text{LiNi}_{0.5}\text{Mn}_{1.5}\text{O}_4$  spinel, with high electrochemical performance was prepared via sol–gel method [7–9], but limited to small-scale production. The effects of substituting manganese ions with other metal ions [10–13] and the partial pressure of oxygen on the structural stability of the spinel [14] were documented recently. The partial substitution of manganese ion improved the cycle stability; however, it resulted in the decrease of the initial reversible capacity. The control of the partial pressure of oxygen was very complicated and difficult to realize in industry. A systematic study on the effect of precursors and mixing methods on the performance of cathodes prepared via solid-state reaction has

been not reported yet. The goal of this work is to study the effect of high energy ball-milling and the effect of various Ni precursors on the electrochemical performance of  $\text{LiNi}_{0.5}\text{Mn}_{1.5}\text{O}_4$  in order to obtain high purity  $\text{LiNi}_{0.5}\text{Mn}_{1.5}\text{O}_4$  spinel using solid-state reaction method.

## 2. Experimental

2.1. Preparation of  $\text{LiNi}_{0.5}\text{Mn}_{1.5}\text{O}_4$ 

$\text{LiNi}_{0.5}\text{Mn}_{1.5}\text{O}_4$  was synthesized by a mechanical activated solid-state reaction from stoichiometric amount of  $\text{Ni}(\text{NO}_3)_2 \cdot 6\text{H}_2\text{O}$ ,  $\text{MnO}_2$  and  $\text{Li}_2\text{CO}_3$ . Precursors were mixed in a ball-milling machine with anhydrous ethanol as dispersion media. The mixture was allowed to ball-mill in a planetary micromill or manual-mixing for 5–12 h. The milled mixture was dried at  $100^\circ\text{C}$  and then calcined at  $750^\circ\text{C}$  for 6–24 h.  $\text{Ni}(\text{CH}_3\text{COO})_2 \cdot 6\text{H}_2\text{O}$ , NiO and  $\text{Ni}_2\text{O}_3$  were also used as Ni resources to prepare  $\text{LiNi}_{0.5}\text{Mn}_{1.5}\text{O}_4$ . The samples made from different Ni resources were listed in Table 1.

## 2.2. Characterization

X-ray phase analysis was carried out on a Rigaku/Max-RA X powder diffractometer with  $\text{Cu K}\alpha$ -radiation. The scan range is  $10 < 2\theta < 70^\circ$ , and a step of 0.02 was used. The voltage and current were 30 kV and 100 mA. The chemical composition of the prepared sample was analyzed using inductively coupled plasma spectroscopy (ICP). The valence state of Mn ion in the prepared sample was determined by iodometry technique as follows.  $\text{N}_2$  gas

\* Corresponding author. Tel.: +86 731 2300781.

E-mail address: [chenzhaoyongcioc@126.com](mailto:chenzhaoyongcioc@126.com) (Z. Chen).

**Table 1**  
Sample made from different Ni resources and mixing methods.

Sample label	Ni resource	Mixing methods
A	Ni(NO <sub>3</sub> ) <sub>2</sub> ·6H <sub>2</sub> O	Ball-milling
A1	Ni(NO <sub>3</sub> ) <sub>2</sub> ·6H <sub>2</sub> O	Manual-mixing
B	Ni(CH <sub>3</sub> COO) <sub>2</sub> ·6H <sub>2</sub> O	Ball-milling
C	NiO	Ball-milling
D	Ni <sub>2</sub> O <sub>3</sub>	Ball-milling

was bubbled in 20 mL of HCl (36%) for 10 min. LiI (500 mg) was dissolved in this HCl solution. Then, the synthesized LiNi<sub>0.5</sub>Mn<sub>1.5</sub>O<sub>4</sub> sample (50 mg) was dissolved into the solution. The titration of the solution containing Mn ions was performed with 0.05 mol dm<sup>-3</sup> Na<sub>2</sub>S<sub>2</sub>O<sub>3</sub> [15].

### 2.3. Charge/discharge test

The resulted LiNi<sub>0.5</sub>Mn<sub>1.5</sub>O<sub>4</sub> was mixed with acetylene black, PVDF (weight ratio of LiNi<sub>0.5</sub>Mn<sub>1.5</sub>O<sub>4</sub>, acetylene black and PVDF is 80:10:10) in NMP onto an Al foil (as current collector). The electrodes were dried and pressed using a hydraulic press. Li-ion secondary cells were assembled using lithium sheet as anode and the above prepared electrode as cathodes. Celgard 2400 was used as separator which was soaked in 1.0 mol L<sup>-1</sup> LiPF<sub>6</sub>/EC + DMC [EC:DMC = 1:1] electrolyte. The cells were assembled in an argon protected glove box. The charge/discharge studies were carried out by using a Land-BTL10 automatic battery test system. If not specified, the charge–discharge test was completed at 3.0–4.9 V and the density of current was 70 mA g<sup>-1</sup>.

## 3. Result and discussion

### 3.1. XRD analysis of LiNi<sub>0.5</sub>Mn<sub>1.5</sub>O<sub>4</sub>

During calcinations of milled mixtures, the partial pressure of oxygen should be controlled very carefully; otherwise, Li<sub>2</sub>MnO<sub>3</sub> or LiMnO<sub>2</sub> would be formed in the sample [5]. This prevents a part of Ni entering the lattice of LiNi<sub>0.5</sub>Mn<sub>1.5</sub>O<sub>4</sub> spinel and thereby forms NiO. In our preparation, all the samples were calcined in air. LiNi<sub>0.5</sub>Mn<sub>1.5</sub>O<sub>4</sub> spinel with only traces of NiO and Li<sub>2</sub>MnO<sub>3</sub> was also obtained without any control of partial pressure of oxygen. The XRD patterns of LiNi<sub>0.5</sub>Mn<sub>1.5</sub>O<sub>4</sub> made from Ni(NO<sub>3</sub>)<sub>2</sub>·6H<sub>2</sub>O, Ni(CH<sub>3</sub>COO)<sub>2</sub>·6H<sub>2</sub>O, NiO and Ni<sub>2</sub>O<sub>3</sub>, which were ball-milled and calcined at the same temperature, were compared in Fig. 1. Among all of them, only does the LiNi<sub>0.5</sub>Mn<sub>1.5</sub>O<sub>4</sub> made from Ni(NO<sub>3</sub>)<sub>2</sub>·6H<sub>2</sub>O show pure spinel structure in contrast to standard pattern (JCPDS

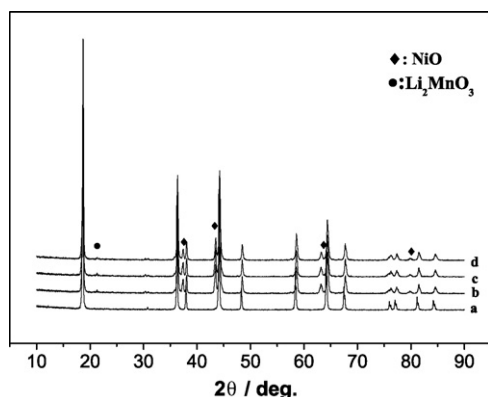


**Fig. 1.** XRD patterns of LiNi<sub>0.5</sub>Mn<sub>1.5</sub>O<sub>4</sub> (a, sample A; b, sample B; c, sample C; d, sample D).

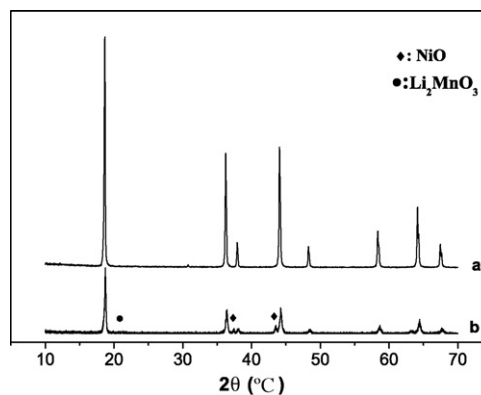


**Fig. 2.** XRD patterns of LiNi<sub>0.5</sub>Mn<sub>1.5</sub>O<sub>4</sub> (a, sample A; b, sample A1).

No. 35-0782). The NiO impurity peaks (JCPDS No. 44-1159) at  $2\theta = 37.5^\circ, 43.5^\circ, 68.2^\circ, 80.0^\circ$  and the Li<sub>2</sub>MnO<sub>3</sub> impurity peak (JCPDS No. 27-1252) around  $2\theta = 21.0^\circ$  were detected in the XRD patterns of all the other LiNi<sub>0.5</sub>Mn<sub>1.5</sub>O<sub>4</sub>, which are very weak impurity peaks. Although there is a trace of NiO and Li<sub>2</sub>MnO<sub>3</sub>, their XRD patterns show standard spinel structure. The amounts of NiO and Li<sub>2</sub>MnO<sub>3</sub> are lower than those reported by Kim et al. [5] using solid-state reaction and very close to the sample prepared via sol-gel method [7]. We presume that there are two reasons why high pure LiNi<sub>0.5</sub>Mn<sub>1.5</sub>O<sub>4</sub> using Ni(NO<sub>3</sub>)<sub>2</sub>·6H<sub>2</sub>O as Ni resource can be prepared with ball-milling. Firstly, the ball-milling could decrease activation energy, which would facilitate the formation of spinel; secondly, the oxygen formed by decomposition of Ni(NO<sub>3</sub>)<sub>2</sub>·6H<sub>2</sub>O would restraint impurity formed in LiNi<sub>0.5</sub>Mn<sub>1.5</sub>O<sub>4</sub>.

XRD patterns of LiNi<sub>0.5</sub>Mn<sub>1.5</sub>O<sub>4</sub>, prepared by ball-milling and manual-milling were shown in Fig. 2. LiNi<sub>0.5</sub>Mn<sub>1.5</sub>O<sub>4</sub> prepared by ball-milling shows pure spinel phase without any impurity peaks in XRD pattern. However, obvious impurity peaks of NiO are noted in the LiNi<sub>0.5</sub>Mn<sub>1.5</sub>O<sub>4</sub> milled manually. Moreover, the intensities of peaks of sample A were much stronger than those of sample A1, which indicated that the ball-milling could facilitate the crystallization of LiNi<sub>0.5</sub>Mn<sub>1.5</sub>O<sub>4</sub>. It is concluded that milling methods have a significant effect on the phase purity of LiNi<sub>0.5</sub>Mn<sub>1.5</sub>O<sub>4</sub>. Through the comparison, the fact was witnessed that better phase purity are obtained is linked to a better mixing of the precursor similarly to soft chemistry routes thus enabling the decrease of ion diffusion length during the synthesis process.

### 3.2. Electrochemical performances of LiNi<sub>0.5</sub>Mn<sub>1.5</sub>O<sub>4</sub>

LiNi<sub>0.5</sub>Mn<sub>1.5</sub>O<sub>4</sub> cathode has two charge/discharge voltage plateaus, i.e., at 4 and 5 V. The plateau at 4 V voltage was caused by Mn<sup>3+</sup>/Mn<sup>4+</sup> redox couple and 5 V plateau by Ni<sup>2+</sup>/Ni<sup>4+</sup>. When there are more Mn<sup>4+</sup> and Ni<sup>2+</sup> in LiNi<sub>0.5</sub>Mn<sub>1.5</sub>O<sub>4</sub>, then the corresponding capacity at 4 V will be less and that at 5 V will be large, and vice versa. Fig. 3a and b shows the charge–discharge voltage profiles of LiNi<sub>0.5</sub>Mn<sub>1.5</sub>O<sub>4</sub> tested at the voltage range of 3.0–5.0 and 3.0–4.9 V, respectively. In Fig. 3a, there is a rapid voltage drop at 4.9 V and then the voltage increases slowly during the course of charge. This could be caused by the oxidation of electrolyte, which will result in abrupt increase of current similar to short circuit of battery. Using this electrolyte, it is better to charge/discharge at the voltage range of 3.0–4.9 V. During the course of test, two charge voltage plateaus were observed at 4.3 and 4.8 V, corresponding to discharge voltage plateaus of 4.0 and 4.6 V. The ratio of corresponding capacities at 4.3 and 4.8 V is 1:2 during charging and 1:1 at 4.0 and 4.6 V during discharging.

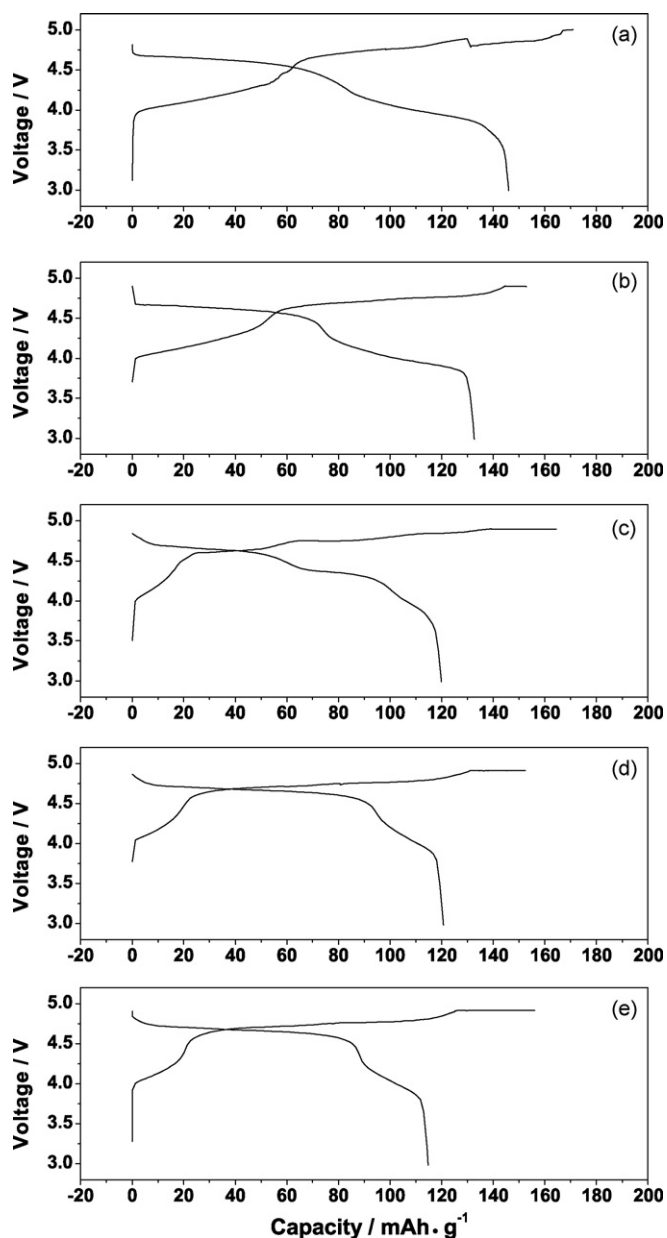


Fig. 3. Initial capacity against voltage (a, sample A, 3.0–5.0 V; b, sample A, 3.0–4.9 V; c, sample B, 3.0–4.9 V; d, sample C, 3.0–4.9 V; e, sample D, 3.0–4.9 V).

In Fig. 3, two discharge voltage plateaus at 4.0 and 4.6 V were observed in sample A, C and D, and it was consistent with Patoux's research [16]. In  $\text{LiNi}_{0.5}\text{Mn}_{1.5}\text{O}_4$ , the 4.0 V discharge voltage plateau corresponds to  $\text{Mn}^{4+} \rightarrow \text{Mn}^{3+}$ , 4.6 V discharge voltage plateau corresponding to  $\text{Ni}^{4+} \rightarrow \text{Ni}^{2+}$ . The voltage profiles of  $\text{LiNi}_{0.5}\text{Mn}_{1.5}\text{O}_4$  made from NiO and  $\text{Ni}_2\text{O}_3$  are similar. The 4.0 V plateau is very small and almost disappeared in comparison with that of sample A. The capacities at 4.6 and 4.0 V plateau are 95 and 15  $\text{mAh g}^{-1}$ , respectively. It is clear that the amount of  $\text{Mn}^{3+}$  decrease, and Mn, Ni trend to form  $\text{Mn}^{4+}$ ,  $\text{Ni}^{2+}$ , when metal oxides were used as Ni resource. Compared with sample A, the initial capacity of  $\text{LiNi}_{0.5}\text{Mn}_{1.5}\text{O}_4$  made from  $\text{Ni}(\text{CH}_3\text{COO})_2 \cdot 6\text{H}_2\text{O}$  (sample B) drops to 120  $\text{mAh g}^{-1}$  (Fig. 3c). A more interesting phenomena appeared, there were three voltage plateaus (at 4.0, 4.4 and 4.6 V) in the discharge voltage profile of sample B, but only two plateaus in sample A. Ratio of corresponding capacities at 4.0, 4.4 and 4.6 V is 1:2:3. The reason of 4.4 V discharge voltage plateau may be attributed to

Table 2

The average oxidation state of manganese of samples and chemical analysis results of  $\text{LiNi}_{0.5}\text{Mn}_{1.5}\text{O}_4$  prepared with different Ni precursors.

Sample label	Average valence state of Mn	Li	Ni	Mn
A	3.85	1.02	0.46	1.47
A1	3.84	1.01	0.54	1.55
B	3.99	0.99	0.3	1.62
C	3.95	0.99	0.47	1.51
D	3.92	0.98	0.5	1.48

the  $\text{Ni}^{3+} \rightarrow \text{Ni}^{2+}$ , 4.6 V corresponding to the  $\text{Ni}^{4+} \rightarrow \text{Ni}^{3+}$ . Amatucci and Kunduraci [17] identified that during the course of discharge, the first  $\text{Ni}^{4+} \rightarrow \text{Ni}^{3+}$  "plateau" lies just above 4.65 V for the ordered P4<sub>3</sub>2 and the later  $\text{Ni}^{3+} \rightarrow \text{Ni}^{2+}$  "plateau" just below 4.65 V for the disordered Fd3m spinels. In our cases, the discharge voltage plateau was 100 mV lower than that reported by Amatucci. It may be because of the higher inner resistance in our man-made half cell. Therefore, only when  $\text{Ni}(\text{CH}_3\text{COO})_2 \cdot 6\text{H}_2\text{O}$  was used as precursor, the  $\text{LiNi}_{0.5}\text{Mn}_{1.5}\text{O}_4$  of disordered Fd3m structure existed. In sample A, the discharge capacity in the 4.0 V discharge voltage plateau was almost 60  $\text{mAh g}^{-1}$ , and it was attributed to a large amount of  $\text{Mn}^{3+}$ , which was confirmed by the average valence state of manganese (Table 2). In the other samples, there was only 30  $\text{mAh g}^{-1}$  in the 4.0 V discharge voltage plateau. The average valence state of manganese in those samples was very close to +4.0. In the chemical composition analysis of all the samples (Table 2), the element contents were a little deviation from the design other than sample A. In sample A, a part of  $\text{Ni}^{2+}$  might be substituted by  $\text{Mn}^{3+}$ , which resulted in a part of  $\text{Mn}^{4+}$  into  $\text{Mn}^{3+}$  in order to keep in electron neutral. As a result, the average valence state of manganese degraded ranging from 4.0 to 3.85. In other samples of B, C and D, there maybe exist a minor part of  $\text{Mn}^{3+}$  and  $\text{Ni}^{3+}$  without carefully control of the partial pressure of oxygen. So, the chemical composition analysis was consistent with the result of the average valence state of manganese and electrochemical performances. There were some capacity above 4.7 V, and it could partly come from electrolyte parasitic reactions.

Fig. 4 shows the variation in the discharge capacity of samples A, as a function of number of cycles at different voltage ranges. The reversible discharge capacity of sample A at 3.0–5.0 V is 11  $\text{mAh g}^{-1}$  higher than that at 3.0–4.9 V. The discharge capacities are up to 145 and 133  $\text{mAh g}^{-1}$  when cut-off voltages are 5.0 and 4.9 V, respectively. It can be seen that the capacity fading is similar for a and b, and the only difference lies in the capacity value. At 3.0–4.9 V, the reversible discharge capacity drops from 133 to 124  $\text{mAh g}^{-1}$  after 40 cycles. At 3.0–5.0 V, sample A shows high stability with the dis-

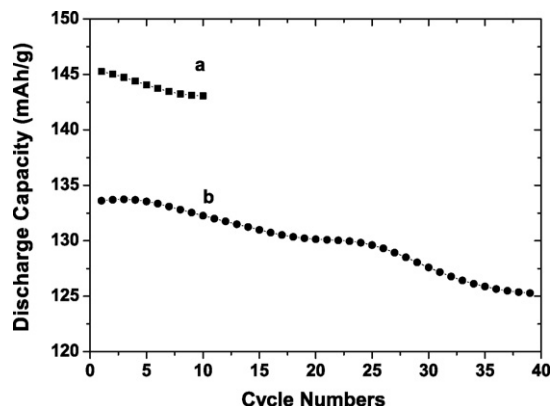


Fig. 4. Capacity vs cycle number of sample A (a: 3.0–5.0 V; b: 3.0–4.9 V).

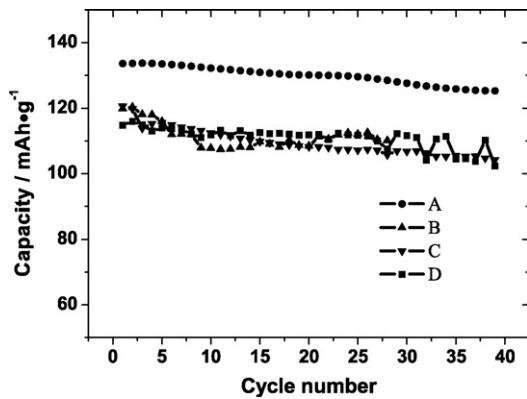


Fig. 5. Capacity against cycle number of sample A, B, C and D (3.0–4.9 V).

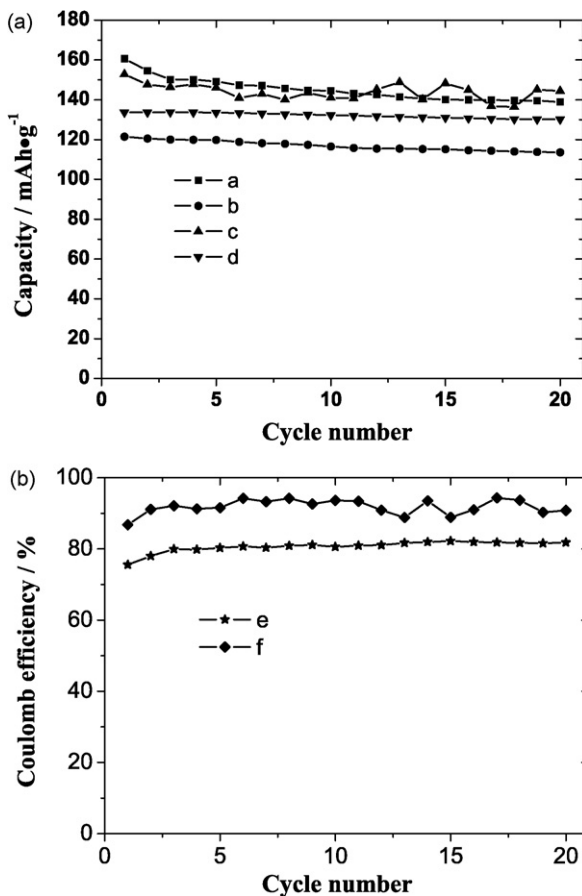


Fig. 6. Capacity and coulomb efficiency against cycle number of sample A and A1 (3.0–4.9 V) (a, b and c, d are respectively charge–discharge cycle curves of sample A1 and A, e, f are respectively coulomb efficiency curves of A1 and A).

charge capacity dropping marginally to  $142 \text{ mAh g}^{-1}$  after 10 cycles. However, at this voltage range, if continuing to be tested, the cell abruptly deteriorated and even unable to be charged because of the decomposition of electrolyte above 4.9 V. So, during the test the charge cut-off voltage was set as 4.9 V.

$\text{LiNi}_{0.5}\text{Mn}_{1.5}\text{O}_4$ , made from various Ni resources also shows excellent stability. The capacity retention rate of sample A, B, C and D were 97.40%, 90.50%, 89.71% and 97.43% respectively (Fig. 5). It showed that the  $\text{LiNi}_{0.5}\text{Mn}_{1.5}\text{O}_4$  made from  $\text{Ni}(\text{NO}_3)_2 \cdot 6\text{H}_2\text{O}$  and  $\text{Ni}_2\text{O}_3$  has good capacity retention rate. The capacity retention rate of  $\text{LiNi}_{0.5}\text{Mn}_{1.5}\text{O}_4$  made from NiO is the lowest.

The effect of milling methods on cycle life and coulomb efficiency of  $\text{LiNi}_{0.5}\text{Mn}_{1.5}\text{O}_4$  made from  $\text{Ni}(\text{NO}_3)_2 \cdot 6\text{H}_2\text{O}$  is shown in Fig. 6. The initial discharge capacity of ball-milled sample is  $12 \text{ mAh g}^{-1}$  higher than that of manual-milled sample. The coulomb efficiency of former is 10% higher than that of latter. The charge capacities of both samples are very close, but there is obvious difference between discharge capacities. It suggests that the Li-ion intercalation/de-intercalation is more reversible in ball-milled sample. The capacity retention rate and stability of ball-milled samples is better than those of manual-milled in the first 20 cycles.

#### 4. Conclusion

$\text{LiNi}_{0.5}\text{Mn}_{1.5}\text{O}_4$  spinel, as a promising cathode material with high reversible capacity and stability has been prepared by solid-state reaction. The phase purity was characterized by XRD. Using  $\text{Ni}(\text{NO}_3)_2 \cdot 6\text{H}_2\text{O}$  as Ni resource and mixing precursors with ball-milling, high pure spinel  $\text{LiNi}_{0.5}\text{Mn}_{1.5}\text{O}_4$  can be prepared via solid-state reaction. Among the  $\text{LiNi}_{0.5}\text{Mn}_{1.5}\text{O}_4$  cathode materials made from various Ni resources, the  $\text{LiNi}_{0.5}\text{Mn}_{1.5}\text{O}_4$  made from  $\text{Ni}(\text{NO}_3)_2 \cdot 6\text{H}_2\text{O}$  has the best electrochemical performance. The  $\text{LiNi}_{0.5}\text{Mn}_{1.5}\text{O}_4$  electrode shows a high initial discharge capacity of  $145 \text{ mAh g}^{-1}$  and a very stable cycling performance. The discharge capacity still retained as  $142 \text{ mAh g}^{-1}$  after 10 cycles. Therefore, it has the potential to substitute currently applied complicated preparation methods like co-precipitation, sol-gel and spray pyrolysis methods for producing high purity  $\text{LiNi}_{0.5}\text{Mn}_{1.5}\text{O}_4$ .

#### Acknowledgment

This work is supported financially by the youth foundation of the department of education of Hunan Province of China (No. 06B002) and the Planned Science and Technology Project of Hunan Province, China (No.2008FJ3008).

#### References

- [1] R. Alcantara, M. Jaraba, P. Lavela, et al., *J. Electrochem. Soc.* 151 (2004) 53–58.
- [2] A. Caballero, L. Hernan, M. Melero, et al., *J. Electrochem. Soc.* 152 (2005) 6–12.
- [3] H. Sang, K. Yang, *Electrochim. Acta* 50 (2004) 431–434.
- [4] A. Eftekhari, *J. Power Sources* 124 (2003) 182–190.
- [5] J. Kim, S. Myung, Y. Sun, *Electrochim. Acta* 49 (2004) 219–227.
- [6] B. Markovsky, Y. Talyossef, G. Salitra, et al., *Electrochem. Commun.* 6 (2004) 821–826.
- [7] S. Yucheng, W. Zhaoxiang, C. Liquan, *J. Power Sources* 132 (2004) 161–165.
- [8] S. Mukerjee, X. Yang, X. Sun, et al., *Electrochim. Acta* 49 (2004) 3373–3382.
- [9] I. Yasushi, N. Hirotsuke, K. Nobuyuki, *J. Power Sources* 119 (2003) 125–129.
- [10] R. Alcantara, M. Jaraba, P. Lavela, et al., *J. Electrochem. Soc.* 152 (2005) 13–18.
- [11] C. Pérez, J. Lloris, J. Tirado, *Electrochim. Acta* 49 (2004) 1963–1967.
- [12] S.H. Oh, S.H. Jeon, W. Cho, C.S. Kim, B.W. Cho, *J. Alloys Compd.* 452 (2008) 389–396.
- [13] C. Locati, U. Lafont, L. Simonin, F. Ooms, E.M. Kelder, *J. Power Sources* 174 (2007) 847–851.
- [14] D. Pasero, N. Reeves, V. Pralong, A.R. West, *J. Electrochem. Soc.* 155 (2008) A282–A291.
- [15] K. Kanamura, W. Hoshikawa, *Solid State Ion.* 177 (2006) 113–119.
- [16] S. Patoux, L. Daniel, C. Bourbon, H. Lignier, C. Pagano, F.L. Cras, S. Jouanneau, S. Martinet, *J. Power Sources* 189 (2009) 344–352.
- [17] M. Kunduraci, G.G. Amatucci, *J. Power Sources* 165 (2007) 359–367.